Increasing the Communication Distance between Nano-biosensing Implants and Wearable Devices

Amit Sangwan, **Honey Pandey**, **Pedram Johari** and **Josep M. Jornet**
Department of Electrical Engineering, University at Buffalo, The State University of New York
Buffalo, NY 14260, USA. E-mail: {amit2, honeypan, pedramjo, jmjornet}@buffalo.edu.

***Abstract*—Significant progress in the fields of electronics, photonics and wireless communications have enabled the development of compact wearable devices, with applications in diverse domains such as fitness, wellness and healthcare. In parallel, nanotechnology is facilitating the development of nano-biosensors, i.e., miniaturized sensors that can be implanted subcutaneously and measure various types of biological events at the nanoscale with unprecedented accuracy. The majority of nano-biosensing systems consist of an external optical excitation and measurement device that can induce and measure the response of implanted optical resonant nano-biosensors. However, the high path-loss of the human body at optical frequencies and the weak response of nano-biosensors would compromise the communication between the body-mounted optical excitation/measurement system and the intra-body implant. In this paper, mechanisms are proposed to overcome the high intra-body path-loss and enable wireless communications with deeper implants. More specifically, the combination of analog beam-forming with optical nano-antenna arrays together with light-guiding hydrogel implants is studied to overcome the spreading loss and to increase the intra-body wireless communication distance. The proposed scheme is analytically modeled and validated through simulations to benchmark its performances against the traditional methods.**

***Index Terms*—Biosensing, wearable communications, intra-body communication, nano-antenna, optical communication.**

I. Introduction

Advancements in the fields of electronics, photonics, and wireless communications have led to the development of compact wearable devices, with applications in varied domains including wellness, fitness, healthcare and security, among others. A report published by the International Data Corporation (IDC) depicts 163.6% increase in the shipments of wearable devices from 28.9 million units in 2014 to 76.1 million in 2015 [1], and it is projected to reach 173.4 million by 2019. Among all the wearable devices, medical devices are dominant and are widely used to provide health associated data [2]. The interconnection of medical wearable devices in Body Area Networks (BANs) [3] forms the basis of innovative healthcare systems. However, in spite of their high potential, the current wearable devices are only used to measure basic parameters, such as breathing, heart rate, blood pressure and temperature.

Alongside this progress, nanotechnology is enabling the development of miniature sensors with critical dimensions below 100 nm that can detect various events occurring at the nanoscale, such as the presence of particular bio-markers with exceptional accuracy. Lately, in-vivo nano-biosensing systems, which operate real time in the human body, have been suggested to provide disease diagnosis and treatment faster and with higher accuracy in comparison to traditional technologies [4]. In this regard, Surface Plasmon Resonance (SPR) sensors have been successfully utilized to monitor circulating biomarkers in blood for the analysis of deadly diseases, ranging from distinct neuronal and cardiovascular diseases [5], [6] to various types of cancer [7], [8]. However, regardless of the possibilities of this technology, there are many limitations in the present systems, such as bulkiness and cost of the excitation and detection systems, which limit the real-world impact. Also, the conventional sensing methods and data collection and processing used are time-consuming, and the lack of timely treatment because of late diagnosis is one of the major causes of poor survivals. These limitations reflect the immediate need for next-generation health monitoring and diagnoses systems to overcome these challenges.

In light of these results, we have recently proposed [9] an architecture to bridge the gap between the two disjoint paradigms, mainly, by shrinking those large SPR-sensing systems to the size of commercial wearable devices and use it with advanced nano-biosensing technologies. The proposed architecture relies on the communication between a passive biosensor (SPR-based nanoplasmonic biochip) implanted subcutaneously in the users body (e.g., wrist) and a nanophotonic wearable smart band, which consists of an array of nano-lasers and nano-photodetectors for excitation and measurement from the implanted biosensor. Despite notable progress from the technology perspective, there are significant communication and signal processing challenges introduced by the nature of the problem. To reliably operate, the nano-biosensors should be implanted under the skin deep enough to be in contact with blood. However, at the same time, the high path-loss of human body at optical frequencies and the weak response of nano-biosensors can pose a challenge for the communication between the body-mounted optical excitation/measurement system and the intra-body implant [10], [11].

In this paper, we propose a novel technique to overcome the high intra-body path-loss and enable wireless communications with deeper implants, with the ultimate goal of increasing the reliability of the in-vivo nano-biosensing systems. More specifically, the combination of analog beam-forming with optical nano-antenna arrays together with light-guiding hydrogel implants is studied to overcome the spreading, absorption and scattering losses and increasing the intra-body wireless communication distance. After summarizing the key aspects in intra-body light propagation, we analytically model and numerically investigate the performance of our proposed scheme in terms of distance gains through simulations and benchmark it against the traditional methods.

The remainder of this paper is organized as follows. In Sec. II, we present our complete system architecture. In Sec. III, the light propagation in biological tissues is studied. In Sec. IV, we discuss the nano-antenna array structure to focus the light. In Sec. V we investigate different approaches

978-1-5386-3512-4/18/$31.00 ©2018 IEEE

to guide the light through biological tissues. In Sec. VI we present the results and benchmark the performance of proposed techniques. Finally, we conclude the paper in Sec. VII.

II. System Model

Our proposed architecture, as illustrated in Fig. 1, is integrated by an implantable SPR-based nano-biosensor implant and a wearable photonic wristband. The smart band (wearable device) consists of the optical signal generators which are the nano-lasers [12]; an array of directivity controlling optical antennas [13]; and a detection and signal processing unit. The sensing implant is a passive device that enables the measurement of certain types of biomarkers in the circulatory system. Sensing of a particular bio-marker happens by the shifts in its refractive index and, eventually, the sensor resonance frequency which is a result of chemical reactions with biomarkers. The generated optical signal in the wearable device is transmitted through an array of optical nano-antennas with a controlled specific beam-pattern to target the precise location of the implant. To overcome the substantial loss in the skin further a light guiding optical waveguide based on a biocompatible hydrogel is used. A multilayer structure is used to model skin tissue [9] behavior. Moreover, the properties such as the scattering, absorption and refractive index specific to different biological tissue layers are used to calculate the channel response.

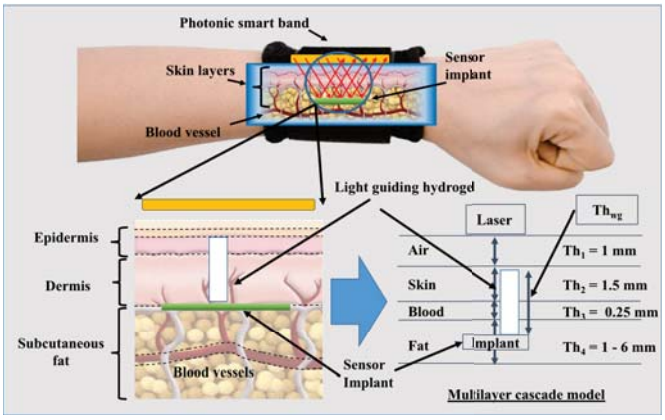

Fig. 1. Multilayer cascade model of skin tissue for wearable to implant communication channel modeling.

III. Light Propagation in Biological Tissues

In this section, we summarize the main properties affecting light propagation in the body [9].

A. Spreading

For spherical free-space propagation of the Electromagnetic (EM) waves, the loss due to spreading can be formulated as:

$$L_{spr} = \frac{1}{D}\left(\frac{4\pi}{\lambda_g^2}\right)\left(4\pi d^2\right), \tag{1}$$

where, $\lambda_g = \lambda/n$ is the effective wavelength, n is the real part of the refractive index, d is the distance from the radiation source and directivity $D = 4\pi/\Omega_A$, where Ω_A is given as:

$$\Omega_A = \int_{\phi=0}^{\Delta\phi}\int_{\theta=0}^{\Delta\theta} sin\theta d\theta d\phi = \Delta\phi(1 - cos\Delta\theta), \tag{2}$$

where θ and ϕ are the azimuth and polar angles in the spherical coordinate system, respectively.

B. Absorption and Scattering

The total attenuation caused by molecular absorption and scattering L_{as} is given by the *Beer-Lambert Law*

$$L_{as} = e^{(\mu_{abs}+\mu_{sca})d}, \tag{3}$$

where μ_{abs}, μ_{sca} are the absorption and scattering coefficients.

C. Reflectance and Transmittance

In addition, we consider the boundary loss which is the intensity attenuation of the EM source when traveling from one media to another. Transmittance $T = 1 - R$ and Reflectance of the light is:

$$R = (|(n_1 - n_2)|/(n_1 + n_2))^2, \tag{4}$$

D. Channel Impulse Response

Considering the above mentioned channel, its response can be obtained as:

$$h(t) = \sum_{i=1}^{N} h_i(t), \tag{5}$$

where N is the number of multipath and $h_i(t) = a_i\delta(t - \tau_i)$ is the channel response of each layer, where a denotes the frequency-dependent attenuation experienced by the light ray is a combination of all the losses given as: $a_i = L_{as,i}L_{spr,i}R_i$, and τ_i is the time delay for each of the rays received form different paths (reflections from different layers).

IV. Use of Nano-antenna Arrays to Focus Light

One of the main challenges for the communication with the implant is the spreading of light inside the tissues that leads to power loss and signal attenuation. This attenuation limits the depth of the implant in the body. From (1) and (2), the spreading loss is proportional to the beam width produced by the antenna; therefore, by focusing the light into a narrower beam, we can allow light to travel more in-depth and to increase the intra-body wireless communication distance. With antenna arrays its possible to focus the EM waves into a beam and at the desired point. Leveraging the reliability and state of the art technology of optical nano-antennas and control strategies for antenna arrays, we can likewise create functional beamforming with an optical nano-antenna array. However, before designing an array, we need to design an antenna element that can resonate and radiate the EM waves at optical wavelengths.

A. Single Element Design of an Optical Nano-Antenna

The design of a plasmonic nano-antenna involves the use of high precision nano-structures and the understanding of the plasmonic properties of noble metals (e.g., gold and silver), which at optical frequencies exhibit complex-value conductivity and allow the propagation of Surface Plasmon Polariton (SPP) waves. Such waves, which appear at the metal-dielectric interface, propagate at a much lower speed than free-space propagating waves. The resulting SPP wavelength, λ_{spp} is consequently smaller than that of free space, λ, leading to the construction of a smaller antenna compared to an "ideal" antennas built with Perfect Electric Conductor (PEC) materials

at the same frequency. As shown in recent studies [13], [14] the resultant length for optical nano-antennas is given by $L_{dipole} = \lambda_{spp}/2$ where $\lambda_{spp} = (2\pi/Re\{k_{spp}\})$, where k_{spp} is SPP wavenumber.

B. Inter-element Spacing Design of a Nano-Antenna Array

In addition to the behavior of each radiating element, the performance of an antenna array also depends on the separation between elements. On the one hand, increasing the separation between two consecutive elements beyond $\lambda/2$ leads to spatial undersampling and, thus, the generation of side lobes. On the other hand, reducing the distance between elements can lead to mutual coupling effects that affect the antenna response. More specifically, mutual coupling between elements results into a change in the antenna input impedance and, thus, resonant frequency (a term known as red-shift or blue-shift in optical terms). In RF antenna arrays, the mutual coupling effects are related to the free-space wavelength. In optical nano-antenna arrays, the minimum inter-element separation depends on the SPP wavelength instead, as we illustrate next by leveraging coupled mode theory.

Couple Mode Theory: The coupling between two antennas and their resonant modes can be described mathematically by coupled mode theory. Typically, a coupled mode model consists of a resonator with an account for its losses (conduction and radiation) and incident waves from outside. From [15], we can represent the amplitude by the following equation:

$$\frac{d\tilde{a}_1}{dt} = (i\omega_1 - \gamma_1 - \Gamma_1)\tilde{a}_1 + ik\tilde{a}_2 + i\sqrt{\gamma_1}(s + i\sqrt{\gamma_2}e^{-ikd}\tilde{a}_2), \quad (6)$$

$$\frac{d\tilde{a}_2}{dt} = (i\omega_2 - \gamma_2 - \Gamma_2)\tilde{a}_2 + ik\tilde{a}_1 + i\sqrt{\gamma_2}(s + i\sqrt{\gamma_1}e^{-ikd}\tilde{a}_1), \quad (7)$$

where a_1 and a_2 are the amplitudes and ω_1 and ω_2 are the resonant (un-coupled) natural frequencies [16]. γ is the radiative loss, Γ is the conductive loss, k is the coupling coefficient and s is the incoming plane wave and $\tilde{a}_{1,2} = a_{1,2}e^{j\omega t}$. To simplify the case, we consider two lossless resonators which do not affect the resonance condition induced by resonance fields. For a very high-frequency system, this separation is very small, and the re-radiation of energy can be assumed to be zero [15]. Therefore, $\Gamma = 0, \gamma = 0$ and $s_+ = 0$, and the equations for the resonators can be given by [17]:

$$\frac{da_1}{dt} = j\omega_1 a_1 + k_{12}a_2, \qquad \frac{da_2}{dt} = j\omega_2 a_2 + k_{21}a_1. \quad (8)$$

This theory works as long as the system is linearly perturbing specially when the terms $k_{12}a_2$ and $k_{21}a_1$ are very small compared to $j\omega_1 a_1$ and $j\omega_2 a_2$. At the optical frequencies, the materials display complex permittivity and conductivity model and the main mode of propagation of waves is the SPP wave. Hence, the size of the antenna and the coupling coefficient will also depend on the SPP wavelength λ_{spp} which is smaller than the free space wavelength making more compact spacing possible and the size of antenna smaller than conventional perfect conductor antennas. The coupling coefficient can be approximated by [17]: $k = \alpha\omega_o e^{-d\beta}$, where ω_o is the resonant frequency without coupling, α and β are tuning constants and d is the separation between elements.

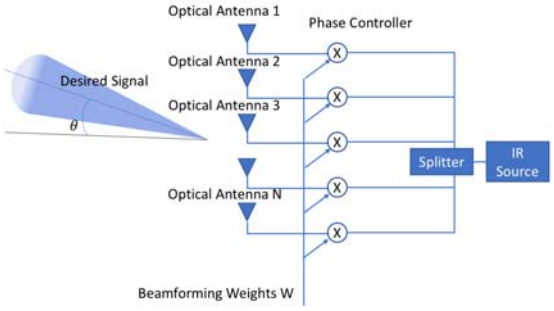

(a) Array Control Architecture 1

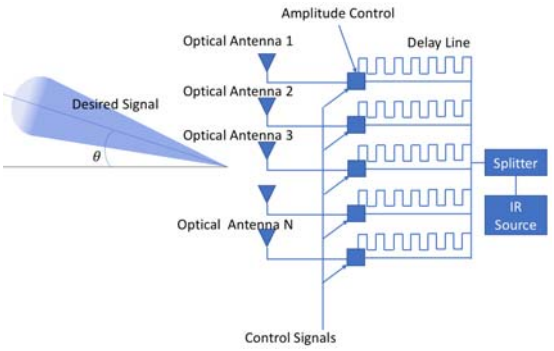

(b) Array Control Architecture 2

Fig. 2. (a) Architecture of the system with common source and unique phase control for each element. (b) Architecture of the system with common source and unique delay line for each element.

C. Optical Nano-antenna Array Control

While using fixed nano-antenna arrays with a predefined beam pattern is possible, the fact that the relative position of the wearable device and the implant can change in time (we cannot expect the user to align the smart band and the implant with micrometric precision) requires the development of control algorithms that support dynamic beamforming. Capabilities and performance of such control algorithms depend on the underlying array architecture. Next, we describe three different architectures which are realizable with the current state of the art in nanophotonics.

1) Antenna Array Architecture 1: Each antenna element is fed through a phase controller: In this architecture, as shown in Fig. 2(a) a single optical signal source (i.e., nano-laser) is utilized to excite an array of optical phase-shifters and optical nano-antennas. Such phase shifters [18], have been experimentally demonstrated and allow the analog control of the SPP wave phase. Please note many of the existing nano-biosensing platforms operate in continuous-wave (single tone) mode. As a result, narrow-band phase-shifters can be utilized efficiently to control the relative phase between radiating elements. As in RF antenna arrays, the weight ω_i at each nano-antenna i can be engineered to allow the beamforming at a particular angle θ_o and ϕ_o, and minimize the side lobes. For example, in a linear (1D) array pointing at desired angle θ_s, the required phase shift between the first and m-th element is given by $\Delta\phi_{s,m} = 2\pi(m-1)d\sin\theta_s/\lambda_c$.

2) Antenna Array Architecture 2: Each element is fed through a delay line: While continuous wave operation of the optical source is common practice in in-vitro / off-body nano-biosensing setups, several reasons motivate the use of

pulsed lasers for in-vivo applications. On the one hand, due to the reflected signal at each tissue layer (Sec. II), the received signal suffers from multi-path propagation, which can mask the rather weak implant response. On the other hand, the continuous operation of the laser can lead to photothermal effects resulting from molecular absorption (Sec. II). Both phenomena can be addressed by utilizing sub-picosecond operated lasers [19]. However, in such case, narrow-band phase shifters cannot effectively control the radiated signals. Instead, as shown in Fig. 2(b) controllable optical delay lines can be utilized [20]. The needed delay for the required phase shift for the steering at angle θ_s can be represented by: $\Delta T = (d(\sin\theta_s))/(v_o)$, where, θ_s is the desired angle for beam, $v_o = c/n$ is the speed of light in the medium of propagation and d is the spacing/distance between the array elements. The corresponding phase shift for this delay, if we assume the carrier signal to be of narrow bandwidth can be denoted by $\Delta\phi = (2\pi d \sin\theta_s)/(\lambda_c)$.

3) Antenna Array Architecture 3: Each element consists of a dedicated light source and delay line: In this design, as shown in Fig. 3 each element in the array consists of a light-source, delay line, and optical nano-antenna. This architecture introduces some challenges, such as the need to operate the different light sources coherently, but also some new opportunities, such as the opportunity to control the weight of each antenna not only in phase but also in amplitude. Indeed, by switching the different light sources ON or OFF, we can manipulate the weight coefficients $|\omega_i| \in \{1, 0\}$.

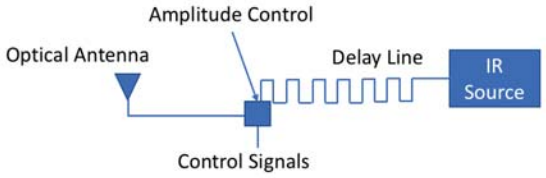

Fig. 3. Array Control Architecture 3: Architecture of the system with one source and delay line for each element.

Performance Gains: Next, we focus on the latter architecture and estimate its performance. In a 2-dimensional NxN array for main beam at $\theta = \theta_o$ and $\psi = \psi_o$ progressive phase difference between elements in x or y-direction can be represented by $\beta = -(2\pi/\gamma)\sin\theta_o\cos\phi_o$, where θ refers to the elevation angle and ϕ refers to azimuthal angle, (θ_o, ϕ_o) is beam pointing direction, γ is the confinement factor and is equal to λ/λ_{spp}. The nano-antenna array radiation diagram is given by the product of the single element radiation diagram by the array factor (AF) [21]:

$$AF(\theta,\phi) = \frac{1}{N}\left(\frac{sin(N\frac{\psi_x}{2})}{sin(\frac{\psi_x}{2})}\right)\frac{1}{N}\left(\frac{sin(N\frac{\psi_y}{2})}{sin(\frac{\psi_y}{2})}\right) \quad (9)$$

For a uniform planar (2D) array, with inter-element separation given by λ_{spp},

$$\begin{aligned}\psi_x &= \frac{2\pi}{\gamma}sin\theta cos\phi - \frac{2\pi}{\gamma}sin\theta_0 cos\phi_0,\\ \psi_y &= \frac{2\pi}{\gamma}sin\theta cos\phi - \frac{2\pi}{\gamma}sin\theta_0 cos\phi_0.\end{aligned} \quad (10)$$

The radiation pattern of the array is given by: $f(\theta,\phi) = E(\theta,\phi)\,AF(\theta,\phi)$, where E is the normalized field pattern of a single element. Hence, the total gain can be given as:

$$Gain_{dB} = 20\log(f(\theta,\phi)). \quad (11)$$

V. Using Hydrogel waveguide

Another approach to overcoming the substantial path-loss in the biological tissues (without increasing the transmission power which may cause photo-thermal damage), is to place a hydrogel waveguide subcutaneously (Fig. 1) to deliver the light to the implanted nano-biosensor. A hydrogel is a low loss material that can be formed synthetically with a variety of reflective indices. In our case, we are interested in a material with higher refractive index than the common human body tissue ($n > 1.47$). This allows for the total internal reflection based channel to guide the light to and from the implant. Hydrogels have been used in tissue engineering to encapsulate cells and as a scaffold to aid the tissue regeneration process. Also, there have been researches where bio-compatible optical fibers with hydrogel core have been developed. One such optical fiber is fabricated by spin coating a low-index Agarose hydrogel ($n = 1.497$) at both sides of a high refractive index Gelatin layer ($n = 1.536$). These optical fibers demonstrated low propagation loss (approximately 0.42 dB/cm for a 1 m long fiber), which makes them suitable for intra-body communication [22]. As shown in Fig. V, for the total internal reflection to occur, the necessary numerical aperture condition for the α is given by: $\sin(\alpha) = \sqrt{\frac{n_2^2+n_3^2}{n_1}}$.

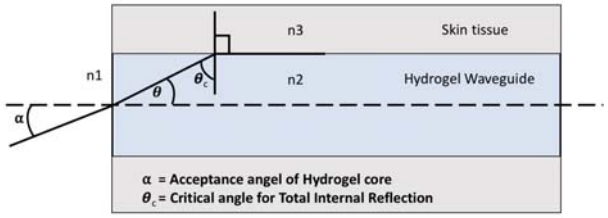

Fig. 4. Numerical aperture for the light to Hydrogel.

VI. Numerical Analysis

In this section, we quantitatively investigate the gains introduced by the aforementioned techniques. First, we plot the antenna array gain given by (11) as function of the number of elements. As observed in the Fig. 5, by increasing the number of elements we can expect an increase in the gain. For a fixed number of elements, an increase in the plasmonic confinement factor leads to a decrease in the gain, because the total extension of the array is then reduced, efficiently reducing the beamforming gain.

In Fig. 6, we illustrate the received power on the wearable device after the reflection at the implant for a transmit power of 100 μW, no transmit or receive gains, receiver sensitivity -100 dBm, and channel model according to the biological tissue model from [9]. An increase from 6.85 mm depth without beamforming gain to 13.65 mm with beamforming gain (55dB) can be achieved using antenna arrays.

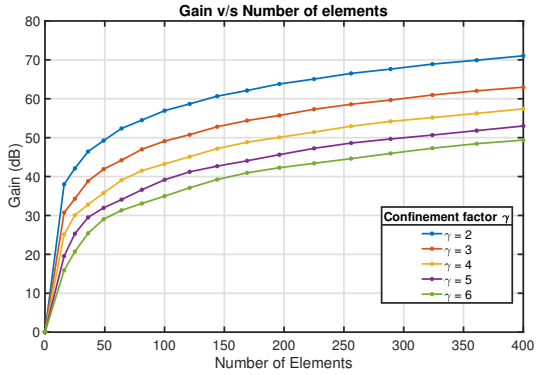

Fig. 5. Antenna array gain vs the number of elements in a NxN array.

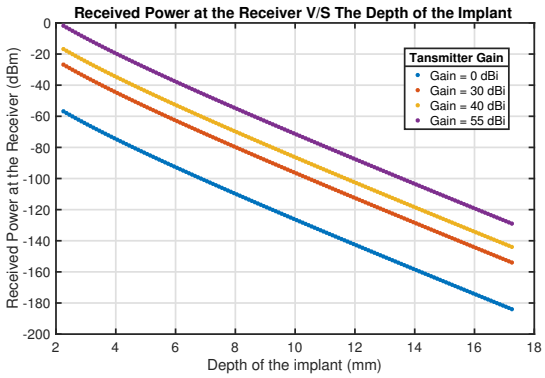

Fig. 6. Change in depth at -100dBm received power with transmitter gain.

Finally, we are interested in calculating the distance gains provided by using the hydrogel implants. Under the assumption of total internal reflection, we can calculate the maximum achievable depth with the total path loss from:

$$L_{air-skin} + L_{hydrogel} - G_{array} = P_{Tx} - P_{Rx}, \qquad (12)$$

where $L_{air-skin}$ is the loss at the air-skin interface, $L_{Hydrogel}$ is the loss in hydrogel medium, G_{BF} is the gain from beamforming, P_{Tx} is the transmitted power and P_{Rx} is the power received by receiver. From [9], we consider the loss at the air-skin interface 31.219 dB, the loss in the hydrogel waveguide 0.42 dB/cm length (transmit power and receiver sensitivity remain unchanged). In Table I, the distance gains for the different configurations are provided. While there will be many challenges in achieving total internal reflection in practical uses of hydrogels, the possibility to utilize light-guiding hydrogels can transform the way wearable and implants communicate.

Configuration	Maximum Implant Depth
Without Beamforming	6.85 mm
With Beamforming (Gain=55dBi)	13.65 mm
With Hydrogel	6995.00 mm
With Hydrogel and Beamforming	13 545.00 mm

TABLE I
MAXIMUM REACHABLE IMPLANT DEPTH WITH DIFFERENT TECHNIQUES

VII. Conclusion

In this paper, different approaches to increase the communication distance between biosensing implants and wearable devices have been discussed and numerically investigated. Optical nano-antenna arrays and beamforming shows an increase in achievable depth of the sensing implants to a few millimeters. However, if the bio-sensing implant needs further depth, the use of light-guiding hydrogel waveguides offers promising results. These numerical results encourage further research concerning optical beamforming as well as system-level optimization.

Acknowledgements

This work was supported by the U.S. National Science Foundation (NSF) under Grant No. IIP-1718177.

References

[1] I. D. C. (IDC), "Worldwide quarterly wearable device tracker," *[Online]. Available: http://www.idc.com/getdoc.jsp?containerId=prUS25903815, Accessed on: January 2016*.
[2] Statista, "Use of wearable devices: Which type of wearable device interests you most?" *[Online]. Available: http://www.statista.com/statistics/259386/us-consumer-interest-in-wearable-computing-devices/, Accessed on: January 2018*.
[3] S. Movassaghi, M. Abolhasan, J. Lipman, D. Smith, and A. Jamalipour, "Wireless body area networks: A survey," *IEEE Communications Surveys & Tutorials*, vol. 16, no. 3, pp. 1658–1686, 2014.
[4] M. A. Eckert and W. Zhao, "Opening windows on new biology and disease mechanisms: development of real-time in vivo sensors," 2013.
[5] C. L. Wong and M. Olivo, "Surface plasmon resonance imaging sensors: a review," *Plasmonics*, vol. 9, no. 4, pp. 809–824, 2014.
[6] H. H. Nguyen, J. Park, S. Kang, and M. Kim, "Surface plasmon resonance: a versatile technique for biosensor applications," *Sensors*, vol. 15, no. 5, pp. 10 481–10 510, 2015.
[7] M. Vendrell, K. K. Maiti, K. Dhaliwal, and Y.-T. Chang, "Surface-enhanced raman scattering in cancer detection and imaging," *Trends in biotechnology*, vol. 31, no. 4, pp. 249–257, 2013.
[8] L. Wu and X. Qu, "Cancer biomarker detection: recent achievements and challenges," *Chemical Society Reviews*, vol. 44, pp. 2963–2997, 2015.
[9] P. Johari, H. Pandey, and J. M. Jornet, "Interconnecting wearable devices with nano-biosensing implants through optical wireless communications," in *International Society for Optics and Photonics, SPIE, Photonics West 2018*, vol. 10501.
[10] P. Johari and J. M. Jornet, "Nanoscale optical wireless channel model for intra-body communications: Geometrical, time, and frequency domain analyses," *IEEE Transactions on Communications*, 2018.
[11] H. Elayan, R. M. Shubair, J. M. Jornet, and P. Johari, "Terahertz channel model and link budget analysis for intrabody nanoscale communication," *IEEE transactions on nanobioscience*, vol. 16, no. 6, pp. 491–503, 2017.
[12] L. Feng, Z. J. Wong, R.-M. Ma, Y. Wang, and X. Zhang, "Single-mode laser by parity-time symmetry breaking," *Science*, vol. 346, no. 6212, pp. 972–975, 2014.
[13] M. Nafari and J. M. Jornet, "Modeling and performance analysis of metallic plasmonic nano-antennas for wireless optical communication in nanonetworks," *IEEE Access*, 2017.
[14] L. Novotny, "Effective wavelength scaling for optical antennas," *Physical Review Letters*, vol. 98, no. 26, p. 266802, 2007.
[15] W. Tan et al., "Manipulating electromagnetic responses of metal wires at the deep subwavelength scale via both near-and far-field couplings," *Applied Physics Letters*, vol. 104, no. 9, p. 091107, 2014.
[16] H. A. Haus, *Waves and fields in optoelectronics*. Prentice-Hall,, 1984.
[17] L. Zakrajsek, E. Einarsson, N. Thawdar, M. Medley, and J. M. Jornet, "Design of graphene-based plasmonic nano-antenna arrays in the presence of mutual coupling," in *EuCAP 2017*. IEEE, 2017, pp. 1381–1385.
[18] D. J. Jones, S. A. Diddams, J. K. Ranka, A. Stentz, R. S. Windeler, J. L. Hall, and S. T. Cundiff, "Carrier-envelope phase control of femtosecond mode-locked lasers and direct optical frequency synthesis," *Science*, vol. 288, no. 5466, pp. 635–639, 2000.
[19] A. Garnache, S. Hoogland, A. Tropper, I. Sagnes, G. Saint-Girons, and J. Roberts, "Sub-500-fs soliton-like pulse in a passively mode-locked broadband surface-emitting laser with 100 mw average power," *Applied Physics Letters*, vol. 80, no. 21, pp. 3892–3894, 2002.
[20] J. Xie, L. Zhou, Z. Li, J. Wang, and J. Chen, "Seven-bit reconfigurable optical true time delay line based on silicon integration," *Optics express*, vol. 22, no. 19, pp. 22 707–22 715, 2014.
[21] C. A. Balanis, *Modern antenna handbook*. John Wiley & Sons, 2011.
[22] M. Choi, J. W. Choi, S. Kim, S. Nizamoglu, S. K. Hahn, and S. H. Yun, "Light-guiding hydrogels for cell-based sensing and optogenetic synthesis in vivo," *Nature photonics*, vol. 7, no. 12, pp. 987–994, 2013.